Syndiotactic Polystyrene/Naphthalene Intercalates: Preparing Thermoreversible Fibrillar Gels from a Solid Solvent

Sudip Malik,[†] Cyrille Rochas,[‡] and Jean Michel Guenet*,[†]

Institut Charles Sadron, CNRS UPR 22, 6 rue Boussingault, BP 40016, F-67083 Strasbourg Cedex, France, and Laboratoire de Spectrométrie Physique, CNRS-UJF UMR5588, 38402 Saint Martin d'Hères Cedex, France

Received December 22, 2004; Revised Manuscript Received February 16, 2005

ABSTRACT: The thermodynamics (temperature−concentration phase diagram), the crystal structure, and the morphology of systems prepared from syndiotactic polystyrene (sPS) in naphthalene, a solvent solid at room temperature, are reported. From the temperature−concentration phase diagram and from neutron diffraction investigations, it is shown that sPS/naphthalene can form two compounds of differing stoichiometries but having the same diffraction pattern. Time-resolved X-ray diffraction experiments are in agreement with the outcomes of the $T-C$ phase diagram. The morphology of these systems is found to be essentially fibrillar and reminiscent of thermoreversible gels obtained from sPS in low-melting-point solvents.

Introduction

Syndiotactic polystyrene (sPS) is a relatively new polymer as its synthesis was only achieved in the late 1980s.[1,2] This polymer has received growing interest as an attractive material due to its high crystallization rate, high melting temperature, low specific gravity, and good chemical resistance.[3] sPS possesses a very complex polymorphic behavior,[4,5] which, for the sake of simplicity, can be described in terms of two crystalline forms, α and β, containing an all-trans conformation with identity period 0.51 nm and two forms, δ and γ, containing a 2_1 helical chain conformation with an identity period of 0.77 nm.[6] sPS has a strong tendency to form polymer−solvent compounds (also designated sometimes as crystallosolvates, intercalates, or chlathrates), which produce the solvated crystalline δ-form with a large variety of solvents such as benzene,[7] toluene,[8] chloroform, bromoform,[9] diethylbenzene,[10] etc. Compound formation is achieved either by exposing solid polymer to liquid solvent or vapor (solvent-induced process)[4,5,11] or by cooling homogeneous solution (solution-cast process).[7,8,12] Interestingly, unlike polyoxyethylene, which produces polymer−solvent intercalates with solvent of melting temperature near or well above room temperature,[13,14] sPS forms complexes with solvent whose melting point can be very low. In the case of toluene, the formation of sPS/toluene compounds occurs while the difference in melting points between the pure polymer and the pure solvent is of about 350 °C. Such conditions are quite exceptional for the formation of compounds where is chiefly involved a recognition process.[13] As mentioned above in the case of poly[oxyethylene] systems, compounds are obtained for solvents whose melting point is, at a maximum, of about 50 °C lower than that of the pure polymer.[13,14] So far, to the best of our knowledge, investigations on sPS systems involving solvents that are solid at room temperature, and thereby systems for which the difference in melting points is significantly lower, are still missing. It is therefore of interest to find out to what extent sPS is also able to form complexes with high-melting-point solvents and, in particular, whether fibrillar systems as those observed in benzene, toluene, chloroform, and the like could also be obtained. Here, we have focused our attention on naphthalene, which in addition to being a solid at room temperature, possesses the propensity to sublimate easily. As will be shown in this paper, fibrillar networks are obtained which can be turned into porous materials through the sublimation of naphthalene. Naphthalene also has a decisive advantage over the aforementioned solvents in that it is far less harmful. In this paper we shall present the temperature−concentration phase diagram for sPS/Naphthalene systems, the resulting morphology, and the structure by time-resolved X-ray diffraction and by neutron diffraction.

Experimental Section

1. Materials. The syndiotactic polystyrene (sPS) samples, hydrogenated (sPSH) and deuterated (sPSD), were synthesized following the method devised by Zambelli and co-workers.[2] The content of syndiotactic triads characterized by ^{1}H NMR was found to be over 99%. The molecular weight characterization of these samples was performed by GPC in dichlorobenzene at 140 °C and yielded the following data: $M_w = 1.0 \times 10^5$ with $M_w/M_n = 4.4$ for sPSH; $M_w = 4.3 \times 10^4$ with $M_w/M_n = 3.6$ for sPSD.

Hydrogenous and deuterated naphthalenes were purchased from Aldrich and were used without further purification.

2. Techniques. *Differential Scanning Calorimetry.* The thermal behavior of the gel was investigated by means of a Perkin-Elmer DSC 7. The systems were systematically melted above 200 °C for 10 min and then cooled to 20 °C at 5 °C/min. The thermograms were recorded with a heating rate of 5 °C/min. The weight of the sample was checked after each experiment, and the instrument was calibrated with indium before each set of experiments.

Two procedures were employed for producing adequate DSC samples. The first procedure was used for polymer fractions lower than $X_{pol} = 0.30$ g/g. Homogeneous solutions were prepared by heating at desired temperature in a hermetically closed test tube that contained a mixture of appropriate amount of polymer and solvent. Gels were obtained by a

[†] CNRS UPR 22.
[‡] CNRS-UJF UMR5588.
* Corresponding author: e-mail guenet@ics.u-strasbg.fr; Tel +33 (0) 388 41 40 87; Fax +33 (0) 388 41 40 99.

10.1021/ma047355d CCC: $30.25
Published on Web 05/07/2005

subsequent cooling of these solutions at room temperature. Pieces of gel were then transferred to into a "volatile sample" pan that was hermetically sealed.

Gels of polymer fractions higher than $X_{pol} = 0.30$ g/g were prepared by allowing evaporation of the solvent from low-concentration sample (typically $X_{pol} = 0.30$ g/g) until the desired polymer fraction was reached as checked by weighing the sample. The samples were introduced into a DSC pan, hermetically sealed, and then subsequently heated to obtain a homogeneous system. To check the reliability of the second procedure, $X_{pol} = 0.30$ and 0.35 g/g samples were prepared by the first procedure. No significant discrepancy was observed between either type of sample.

Also, for some samples kinetic effects were evaluated by using different cooling and heating rates.

Scanning Electron Microscopy. A Hitachi S-2300 operating at a voltage ranging from 15 to 25 kV was used. A film of sPS/naphthalene system was dried in a vacuum at room temperature, and it was coated with a gold layer of thickness 40 nm by the sputtering technique in an argon atmosphere.

Atomic Force Microscopy. AFM experiments were carried out at room sample in air using a Nanoscope III instrument (Digital Instruments, Santa Barbara, CA). The image was taken by means of tapping mode with a silicon nitride cantilever (Scientec, France) having a spring constant of 25−50 N/m and a rotating frequency of 280−365 kHz. Films were prepared by deposition of a drop of hot, homogeneous solution onto a glass slide, and then the solvent was allowed to sublimate. The observation of the surface topography of the films was performed with a scannning rate varying from 1 to 2 Hz.

X-ray Diffraction. The X-ray experiments were performed on beamline BM2 at the European Synchrotron Radiation Facility (ESRF), Grenoble, France. The energy of the beam was 15.8 keV, which corresponds to a wavelength of $\lambda = 7.86 \times 10^{-2}$ nm. At the sample position the collimated beam was focused with a typical cross section of 0.1×0.3 mm^2. The scattered photons were collected onto a two-dimensional CCD detector developed by Princeton Instruments, presently Roper Scientific. Typical acquisition times are about 10−20 s, which allows time-resolved experiments to be carried out at 2 °C/min, a value close to the 5 °C/min heating rate used for DSC experiments.

The sample-to-detector distance was about 0.2 m, corresponding to a momentum transfer vector q range of $1 < q$ (nm^{-1}) < 17, with $q = (4\pi/\lambda)\sin(\theta/2)$, where λ and θ are the wavelength and the scattering angle, respectively (further information is available on the Web site http://www.esrf.fr).

The scattering intensities obtained were corrected for the detector response, the dark current, the empty cell, the sample transmission, and the sample thickness. To obtain a one-dimensional X-ray pattern out of the two-dimensional digitalized pictures, the data were radially regrouped and a silver behonate sample was used for determining the actual values of the momenta transfer q.

A cylinder-like sample 1 mm thick and of 4 mm diameter cut off from a larger sample was placed into the central hole of a 1 mm thick circular aluminum sample holder, both sides of which were eventually covered with 25 μm thick mica foils that were glued with temperature-resistant epoxy resin in order to prevent solvent evaporation which was a very crucial event because of two reasons: (a) it was harmful to the detector, and (b) it could change the sample concentration during the temperature-dependent experiment.

Neutron Diffraction. Neutron diffraction experiments were carried out on D16, a two-circle diffractometer located at Institut Laue Langevin, Grenoble, France. This diffractometer is equipped with a position-sensitive ^{3}He multidetector with 128×128 wires. It operates at a wavelength $\lambda = 0.454$ nm obtained by diffraction of the neutron beam onto a pyrolytic graphite mosaic crystal (mosaicity = 0.7°) oriented under Bragg conditions (further details available at http://www.ill.fr). Momenta transfer $q = (4\pi/\lambda)\sin(\theta/2)$ ranged from $q = 2$ to 12 nm^{-1}. Detector calibration and correction for cell efficiency were achieved by using a light water sample.

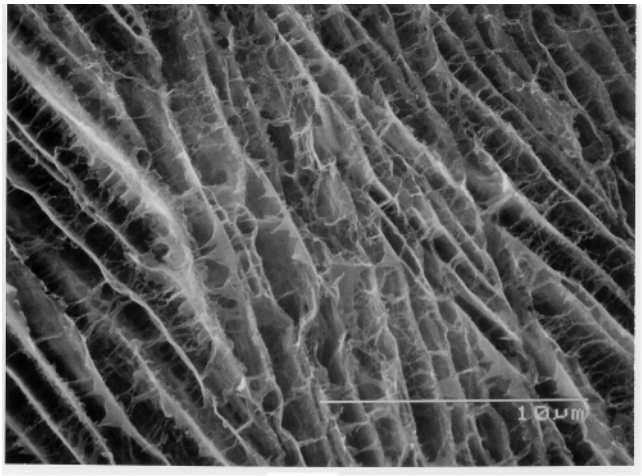

(a)

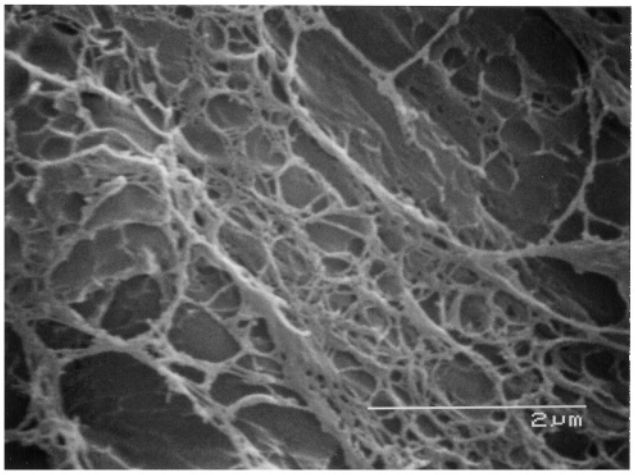

(b)

Figure 1. Scanning electron micrograph of sPS−naphthalene dried gels: (a) $X_{pol} = 0.10$ g/g and (b) $X_{pol} = 0.30$ g/g.

The compounds were prepared directly in amorphous quartz tubes of 3 mm inner diameter. After introducing a mixture of polymer and solvent, these tubes were sealed from the atmosphere. Homogeneous solutions were obtained by heating and then were quenched to room temperature.

Results and Discussion

I. Morphology. The surface morphology of sPS/naphthalene systems has been observed by SEM and AFM techniques. In all cases the solvent has been sublimated beforehand. The morphology features of this system depends markedly on the polymer fraction X_{pol} as two regimes can be identified on either side of a polymer fraction of about $X_{pol} \approx 0.15$ g/g.

At low fractions of sPS (Figure 1a), namely for $X_{pol} \leq 0.10$ g/g, one observes rows of polymer lamellae that are interconnected with fibrils whose diameters are in the range 20−50 nm. Most probably, the lamellar structure of the polymer arises from the shearing produced through the crystallization of the solvent. Possibly, solvent crystallization, which occurs within an already crystallized polymer matrix, creates crystalline polymer platelets. In doing so, it also stretches chains belonging to two adjacent platelets and hence the formation of fibrils.

Above $X_{pol} = 0.20$ g/g the lamellar structures vanish, and only a fibrillar network morphology (Figure 1b) is

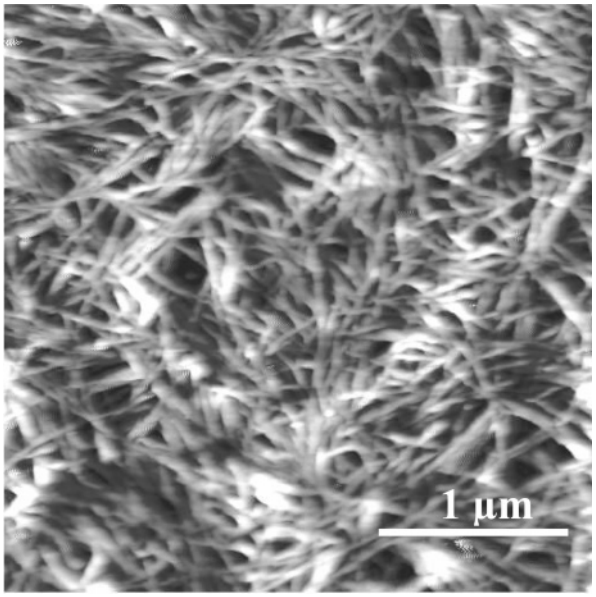

Figure 2. AFM images of sPS−naphthalene gel, X_{pol} = 0.25 g/g.

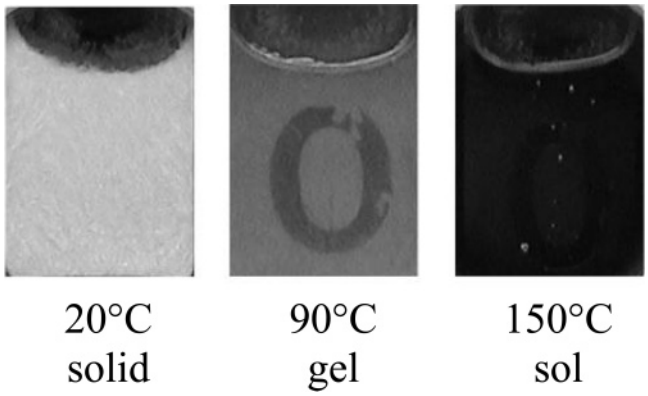

Figure 3. Photograph of X_{pol} = 0.20 g/g sPS−naphthalene gel in 1 mm quartz cuvette against a black background. At 20 °C the system is strongly turbid; at 90 °C it becomes transparent yet slightly turbid as shown by the black mark (**O**) stuck at the rear of the cuvette; above the terminal melting temperature the black mark merges with the black background indicating total transparency.

obtained. Manifestly, above this polymer fraction the solvent crystallization has no impact on polymer morphology. AFM investigations (Figure 2) also reveal the same fibrillar morphology with fibrils possessing an average diameter of about 50 nm. Clearly, here is observed a thermoreversible gel morphology as has been described by Daniel et al.[15] These microscopic features are also indirectly revealed by visual inspection of the samples. As can be shown in Figure 3, sPS/naphthalene samples are whitish and highly turbid at room temperature but become transparent above the melting temperature of naphthalene (82 °C) exactly as are gels of sPS/benzene, iPS/decalin, agarose/water, and the like.[16]

II. Thermodynamics: Phase Diagrams. Typical differential scanning calorimetry (DSC) thermograms of sPS/naphthalene systems obtained at 5 °C/min are shown in Figure 4a for different polymer fractions corresponding to salient thermal events. Two domains can be distinguished: a low-temperature region, typically near 82 °C, where the melting endotherms are related to the only naphthalene, and a high-temperature region dealing with thermal events related to the

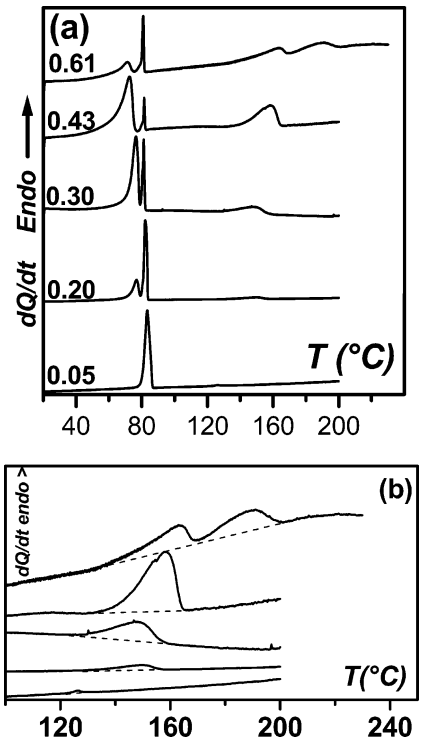

Figure 4. (a) Typical DSC traces of sPS/naphthalene systems at indicated polymer fractions. (b) The expanded portion of the high-temperature domain for the same concentrations.

polymer structures. As the melting enthalpies associated with these events differ by at least 1 order of magnitude, the high-temperature domain has been redrawn in Figure 4b with an expanded scale for the ordinate axis. Note that no kinetic effects are observed when using different heating rates and cooling rates.

As said above, in the low-temperature domain one observes the melting of the free naphthalene present in the system. It is worth noticing that the naphthalene melting consists of two endotherms in the temperature range 82−68 °C for polymer fractions above X_{pol} > 0.20 g/g. The reason for the splitting of the solvent peak in two endotherms is probably due to the fact that increasing polymer fraction produces smaller and smaller free solvent domains. In accordance with Gibbs theory, these domains should display a melting point lower than that of infinite crystals. Note that the first endotherm is broad and reflects the existence of a size distribution of the crystal domains. To be sure, there is still the peak due to infinite crystals but to a much lower extent compared to the first endotherm. This means that the size distribution is not continuous from infinite crystals down to very small crystals. We shall come back to this point later as it may have some bearing with the formation of sPS/naphthalene compounds of differing stoichiometries.

In the high-temperature domain related to polymer melting, one melting endotherm (low-melting endotherm) is observed up to a polymer fraction X_{pol} = 0.50 g/g while for the high-concentration systems a second melting endotherm (high-melting endotherm) appears at higher temperature. The temperature associated with the low-melting endotherm displays a rather sharp increase near X_{pol} = 0.20 g/g. The temperature associated with the high-melting endotherm increases continuously with increasing fractions of sPS investigated here. We further note that, unlike *trans*-decalin, no

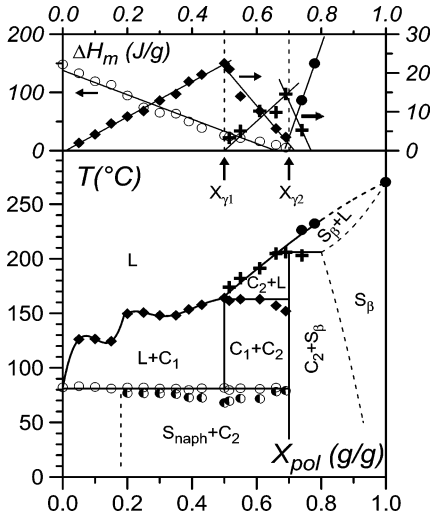

Figure 5. Temperature−concentration phase diagram together with Tamman's diagram for sPS/naphthalene systems. C_1 and C_2 stand for two different compounds of stoichiometries 4/5 and 1/3 (molecules of solvent per monomer), respectively. S_β corresponds to a solid polymer solution consisting of the β-form. Indications in brackets (2_1) and (β) stand for the solvated 2-fold helical form and for the nonsolvated planar zigzag form, respectively. $X_{\gamma 1}$ and $X_{\gamma 2}$ are the compositions of compound C_1 and compound C_2, respectively. The same symbols are used for the first-order transition events and the corresponding enthalpies. Lines joining melting events, except straight lines, are guides for the eyes. Open circles stand for the terminal melting of naphthalene, while half-filled circles stand for the maximum of the broad first endotherm related to the melting of small naphthalene crystals. For the total melting enthalpy of the solvent open circles have been used.

exotherm is seen between the two endotherms. According to Guenet,[17] the exotherm observed with sPS/*trans*-decalin systems in a large range of polymer fractions ($X_{pol} = 0.25-0.7$) arises from the transformation of the nonsolvated 2_1 helix, which is metastable, into the planar zigzag form. The absence of exotherm therefore suggests that one is still dealing with a solvated form of the 2_1 helix and accordingly with a sPS/naphthalene compound.

These results are summarized in the temperature−concentration phase diagram drawn in Figure 5. Also, the variations of the enthalpies associated with each endotherm as a function of polymer fraction are presented in the same figure (Tamman's diagram). Note that the absence of kinetic effects, and also the fact that enthalpies vary linearly, allows the use of the Tamman's diagram to determine the compositions of the various phases as is customary.[18]

The enthalpy variations together with the characteristic shape of phase diagram are consistent with the existence of the two compounds C_1 and C_2 of different stoichiometries. C_1 appears to be a singularly melting compound. Interestingly, C_1 transforms into another compound C_2 both by cooling at low temperature (when naphthalene crystallizes) in a polymer fraction range $0 < X_{pol} < 0.5$ and by heating at high temperature ($T \approx 160$ °C) in a polymer fraction range $0.5 < X_{pol} < 0.7$. From the Tamman's diagram, the stoichiometry of the compound C_1 corresponds to the maximum of the enthalpy associated with the melting and transformation of the compound (Figure 5), namely at $X_{\gamma 1} = 0.5$, which yields about 4 naphthalene molecules per 5 monomer units.

Compound C_2 is of the incongruently melting type. The stoichiometry of compound C_2 is obtained from both

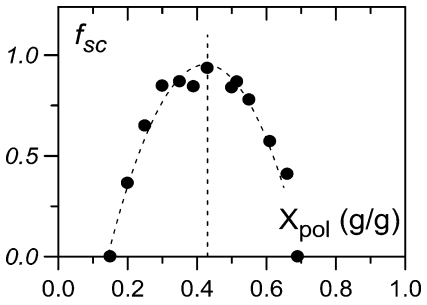

Figure 6. Plot of the ratio (f_{sc}) of the enthalpy of the broad low-melting endotherm with respect to the total naphthalene melting enthalpy vs polymer fraction, X_{pol}.

the polymer fraction at which free naphthalene molecules no longer remain in the system[18] and the polymer fraction at which the melting enthalpy of compound C_2 goes through a maximum. This eventually gives $X_{\gamma 2} = 0.7 \pm 0.02$, which corresponds to about 1 naphthalene molecule per 3 monomer units. This stoichiometry is slightly larger than that reported by Chatani and coworkers[19] for the sPS−toluene system (1 naphthalene molecule per 4 monomer units).

Before discussing further, it is worth belaboring again on the events occurring while crystallizing naphthalene. The transformation from one compound to another while crystallizing the solvent has already been observed for sPS/benzene systems.[7] It indicates that part of the solvent in compound C_1 is loosely bound.[7] If the two-melting endotherms arising from crystallized naphthalene are taken into account (the first, broad endotherm and the second, narrow endotherm), then a linear variation of the melting enthalpy is observed, which eventually becomes zero at $X_{pol} = 0.7$ (Figure 5). This value corresponds to the stoichiometric composition of compound C_2. Alternatively, it is worth considering the ratio of the melting enthalpy associated with the first, broad endotherm with respect to the total naphthalene melting enthalpy (see Figure 6). This ratio goes through a maximum at about $X_{pol} = 0.43 \pm 0.05$. Note that, unlike the total naphthalene melting enthalpy, there is no argument to have a linear behavior. It turns out that this value for the polymer fraction corresponds approximately to the stoichiometric fraction of compound C_1. This suggests that the loosely bound solvent forms small crystallites but is immediately reincorporated into the crystalline lattice at the solvent melting point.

Beyond $X_{pol} = 0.7$ g/g the system consists of compound C_2 and a solid-phase S_β (namely, no solvent molecules participating in the crystalline lattice). As will be discovered in what follows, this solid-phase S_β consists of the β-form of sPS.

It is worth emphasizing that the data from the phase diagram are self-consistent. As a matter of fact, the stoichiometries are obtained both from maxima and from minima of the enthalpies associated with the different thermal events. The phase diagram clearly indicates the existence of two compounds. Finally, it is worth noting that naphthalene and *trans*-decalin[17] produce totally different phase diagrams and correspondingly differing compounds.

III. Structure. a. X-ray Time-Resolved Diffraction. The crystalline structure of the different phases has been studied by X-ray diffraction either as a function of polymer fraction at a fixed temperature or by time-resolved experiments at increasing temperature

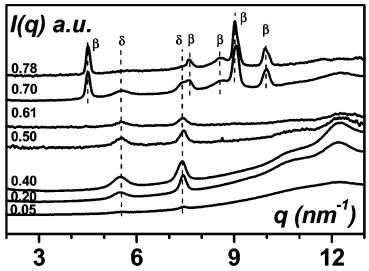

Figure 7. X-ray diffraction patterns of sPS/naphthalene systems at the indicated polymer fraction. Acquisition times of 10 s and heating rate of 2 °C/min. The main reflections of the δ-form and the β-form are shown.

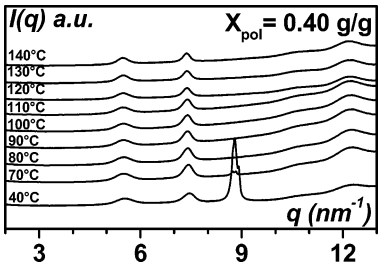

Figure 8. X-ray diffraction patterns of the sPS/naphthalene system for $X_{pol} = 0.40$ g/g. Acquisition times of 10 s and heating rate of 2 °C/min. The strong peak at 8.8 nm^{-1} arises from the free, crystallized naphthalene, and it vanishes upon heating the system above 80 °C.

with a rate of 2 °C/min. The different polymer fractions studied have been chosen on the basis of the outcomes of the temperature−concentration phase diagram.

The X-ray diffraction patterns presented in Figure 7 have been recorded for six different polymer fractions at 90 °C to avoid the very intense peak of naphthalene crystals. The intense reflections seen up to $X_{pol} = 0.61$ at $q = 5.5 \pm 0.1$ nm^{-1} ($d = 1.14 \pm 0.02$ nm) and $q = 7.4 \pm 0.1$ nm^{-1} ($d = 0.85 \pm 0.01$ nm) are characteristic peaks for the δ-form of sPS.[19] At a polymer fraction $X_{pol} = 0.70$ and $X_{pol} = 0.78$, the reflections at $q = 4.5 \pm 0.1$ nm^{-1} ($d = 1.40 \pm 0.02$ nm), 7.6 ± 0.1 nm^{-1} ($d = 0.83 \pm 0.01$ nm), 8.6 ± 0.1 nm^{-1} ($d = 0.73 \pm 0.01$ nm), 9.0 ± 0.1 nm^{-1} ($d = 0.7 \pm 0.01$ nm), and 10.0 ± 0.1 nm^{-1} ($d = 0.63 \pm 0.01$ nm) clearly indicate the overwhelming presence of the β-form of sPS,[6] although reflections of the δ-form, admittedly rather weak, are still observed.

These results show that there is no difference, as far as the diffraction pattern is concerned, in the concentration range from $X_{pol} = 0.05$ to $X_{pol} = 0.61$ although the two different compounds C_1 and C_2 are involved. Clearly, the only difference lies in the value of their stoichiometries.

In Figure 8, time-resolved diffraction patterns of the sPS/naphthalene system at a polymer fraction $X_{pol} = 0.40$ are shown. Here sPS crystalline form corresponds to the δ-form at all temperature. Note that for temperatures below 80 °C the strong reflection at $q = 8.8 \pm 0.1$ nm^{-1} arises from crystallized naphthalene which vanishes upon heating the system above 80 °C. In Figure 9, the time-resolved diffraction patterns of the sPS/naphthalene system for a polymer fraction $X_{pol} = 0.78$ are presented. The reflections at $q = 4.5 \pm 0.1$ nm^{-1}, $q = 7.6 \pm 0.1$ nm^{-1}, $q = 9.0 \pm 0.1$ nm^{-1}, $q = 10.0 \pm 0.1$ nm^{-1}, etc., are all characteristics of the β-form. By carefully inspecting Figure 8, one still notices the presence of the reflection at $q = 7.4 \pm 0.1$ nm^{-1} up to $T = 150-160$ °C, but it is rather weak compared to the

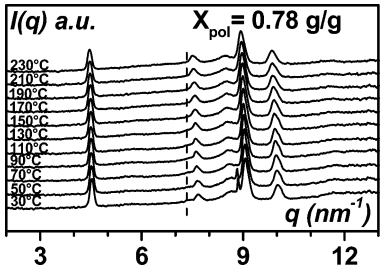

Figure 9. X-ray diffraction patterns of sPS/naphthalene system for $X_{pol} = 0.78$ g/g. Acquisition times of 10 s and heating rate of 2 °C/min. The dashed line at $q = 7.4$ nm^{-1} ($d = 0.85$ nm $\pm$ 0.01) highlights the presence of the δ-form at low temperature.

β-form reflections. This is consistent with the phase diagram where the disappearance of the δ-form is expected to take place in this temperature range for this polymer fraction. A conformational change from the 2_1 helix to planar zigzag is taking place here, as was observed by Rastogi et al.[20] No transformation of the δ-form into the solvent-free γ-form, namely without conformational change, is therefore observed unlike what was reported by several authors[21,22] for other sPS/solvent systems.

b. Neutron Diffraction. Neutron diffraction can be an appropriate investigation tool for systems involving polymer−solvent compounds thanks to the deuterium-labeling possibility of either component. When dealing with a binary system, four labeling possibilities are accessible which provides one with four structure factors without significantly changing the molecular arrangement. The existence of polymer−solvent compounds can be demonstrated qualitatively by this technique,[23,24] as is illustrated by the general expression for the intensity diffracted by a binary system composed of one type of polymer and one type of solvent:

$$I(q) = \bar{A}_p^2(q)\, S_p(q) + \bar{A}_s^2(q)\, S_s(q) + 2A_p(q)\, A_s(q)\, S_{ps}(q) \quad (1)$$

where $A(q)$ and $S(q)$ with appropriate subscripts are the coherent scattering amplitude and the structure factor of the polymer (p) and of the solvent (s), and $S_{ps}(q)$ is a cross-term which is related to the coorganization of the polymer and the solvent. This term is only meaningful when polymer−solvent compounds are dealt with. Changing the labeling of the solvent while keeping the polymer labeling the same generally results in an alteration of the ratio of the intensities of the diffraction peaks related to the compound. Conversely, if no complex is formed, this cross-term vanishes so that the reflections arising from the crystallized polymer are independent of the solvent labeling.

Here we shall discuss only the qualitative aspects of the diffraction patterns that are presented in Figure 10 and Figure 11 for $X_{pol} = 0.20$ and $X_{pol} = 0.73$, respectively. As can be seen in Figure 10, the intensities ratio does vary with the solvent labeling. For instance, the reflection at $q = 7.3 \pm 0.1$ nm^{-1} (indicated by arrow) is much stronger for sPSD/naphthaleneD than for sPSD/naphthaleneH. This clearly supports the existence of a sPS/naphthalene compound. The strong reflection at $q = 8.7 \pm 0.1$ nm^{-1} is due to the free crystallized naphthalene, and it vanishes when the system is heated above 80 °C. In Figure 11 where $X_{pol} = 0.73$ the relative intensities of the peaks at $q = 5.4 \pm 0.1$ nm^{-1} and $q =$

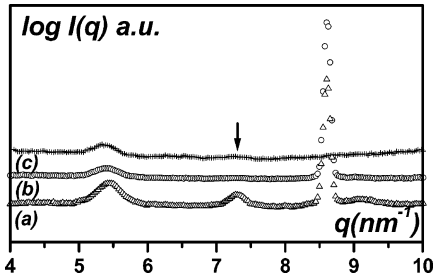

Figure 10. Neutron diffraction pattern for sPS/naphthalene system at $X_{pol} = 0.20$ g/g for different isotopic labeling: (a) sPSD/NaphD at 20 °C, (b) sPSD/NaphH at 20 °C, and (c) sPSD/NaphH at 90 °C. The arrow highlights the effect of the solvent labeling on the reflection at 7.7 nm^{-1}. Note that the strong reflection at 8.7 nm^{-1} arises from the free, crystallized naphthalene, and it vanishes when the system is heated above 80 °C (curve c).

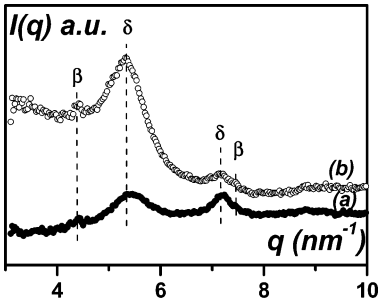

Figure 11. Neutron diffraction pattern for the sPS/naphthalene system for $X_{pol} = 0.73$ g/g for different isotopic labeling: (a) sPSD/NaphD and (b) sPSD/NaphH. The characteristic reflections of the δ-form and of the β-form are highlighted.

7.3 ± 0.1 nm^{-1} depend on solvent labeling, which indicates the presence of another compound at this polymer fraction. Reflections due to the β-form are also present, albeit weak. These results are consistent with the phase diagram that suggests the existence of a compound structure at this concentration together with a small amount of solid-phase S_β.

Concluding Remarks

The temperature−concentration phase diagram for sPS/naphthalene systems has been established, the structure and morphology observed for different polymer fractions. All the results are consistent with the formation of compounds with this solvent solid at room temperature. Interestingly, the morphology is fibrillar as that obtained with benzene. Naphthalene is certainly less harmful than benzene, so that if fibrillar morphology is to be produced, this solvent is more appropriate, the more so as it displays an interesting sublimation tendency. Finally, it is worth emphasizing that compounds can be obtained with a solvent of a molecular volume larger than those mentioned in the Introduction, and yet the diffraction pattern remains virtually unaltered. If naphthalene molecules are to be intercalated the same way as that proposed by Chatani et al. for toluene,[19] the lattice parameter should be expected to vary noticeably and the position of the diffraction peaks as well. Also, the stoichiometry of 0.8/1 leads to a density of 1.78 g/cm^3 and that of 0.3/1 to 1.23 g/cm^3 by considering Chatani's lattice. The stoichiometry problem has already been raised.[17,25] Is the stoichiometry derived from the phase diagram overestimated, or does there exist another possible crystalline lattice that would reconcile the experimental results? In our opinion, this still remains an open question.

Acknowledgment. IFCPAR-CEFIPRA is gratefully acknowledged for financial support of the work (Grant No. 2808-2). Sudip Malik is also indebted to IFCPAR-CEFIPRA (Grant No. 2808-2) for a postdoctoral fellowship. The time-resolved X-ray experiments have been carried out on the French beamline CRG-D2AM at ESRF, while the neutron diffraction investigations have been performed on D16 at ILL (both located in Grenoble, France). The authors are also greatly indebted for experimental assistance to Bruno Deme on D16, to C. Straupé for SEM, and to S. Zehnacker for DSC.

References and Notes

(1) Ishihara, N.; Seimiya, T.; Kuramoto, M.; Uoi, M. *Macromolecules* **1986**, *19*, 2465.
(2) Grassi, A.; Pellechia, P.; Longo, P.; Zambelli, A. *Gazz. Chim. Ital.* **1987**, *117*, 249.
(3) Malanga, M. *Adv. Mater.* **2002**, *12*, 1869.
(4) Immirzi, A.; de Candia, F.; Ianelli, P.; Zambelli, A.; Vittoria, V. *Makromol. Chem. Rapid Commun.* **1988**, *9*, 761.
(5) Vittoria, V.; de Candia, F.; Ianelli, P.; Immirzi, A. *Makromol. Chem. Rapid Commun.* **1988**, *9*, 765.
(6) Guerra, G.; Vitagliano, V. M.; De Rosa, C.; Petraccone, V.; Corradini, P. *Macromolecules* **1990**, *23*, 1539.
(7) Daniel, C.; De Luca, M. D.; Brulet, A.; Menelle, A.; Guenet, J. M. *Polymer* **1996**, *37*, 1273.
(8) Daniel, C.; Brulet, A.; Menelle, A.; Guenet, J. M. *Polymer* **1997**, *38*, 4193.
(9) Rudder, J. D.; Berghmans, H.; Schryver, F. C. D.; Basco, M.; Paoletti, S. *Macromolecules* **2002**, *35*, 9529.
(10) Moyses, S.; Sonntag, P.; Spells, S. J.; Laveix, O. *Polymer* **1998**, *39*, 3665.
(11) Ray, B.; Elhasri, S.; Thierry, A.; Marie, P.; Guenet, J. M. *Macromolecules* **2002**, *35*, 9730.
(12) Malik, S.; Nandi, A. K. *Macromolecules* **2001**, *34*, 275.
(13) Point, J. J.; Coutelier, C. *J. Polym. Sci., Polym. Phys. Ed.* **1985**, *23*, 231.
(14) Dosière, M. *Macromol. Symp.* **1997**, *114*, 63.
(15) Daniel, C.; Dammer, C.; Guenet, J. M. *Polymer* **1994**, *35*, 4243.
(16) Guenet, J. M. In *Thermoreversible Gelation of Polymers and Biopolymers*; Academic Press: London, 1992.
(17) Guenet, J. M. *Macromol. Symp.* **2003**, *203*, 1.
(18) Klein, M.; Guenet, J. M. *Macromolecules* **1989**, *22*, 3716. Guenet, J. M. *Thermochim. Acta* **1996**, *284*, 67. Carbonnel, L.; Guieu, R.; Rosso, J. C. *Bull. Soc. Chim.* **1970**, *8/9*, 2855. Rosso, J. C.; Guieu, R.; Ponge, C.; Carbonnel, L. *Bull. Soc. Chim.* **1973**, *9−10*, 2780.
(19) Chatani, Y.; Shimane, Y.; Inagaki, T.; Ijitsu, T.; Yukinari, T.; Shikuma, H. *Polymer* **1993**, *34*, 1620.
(20) Rastogi, S.; Goossens, J. G. P.; Lemstra, P. J. *Macromolecules* **1998**, *31*, 2983.
(21) Wang, Y. K.; Savage, J. D.; Yang, D. C.; Hsu, S. L. *Macromolecules* **1992**, *25*, 3659.
(22) Yoshika, A.; Tashiro, K. *Macromolecules* **2003**, *36*, 3001.
(23) Klein, M.; Menelle, A.; Mathis, A.; Guenet, J.-M. *Macromolecules* **1990**, *23*, 4591.
(24) Point, J. J.; Damman, P.; Guenet, J.-M. *Polym. Commun.* **1991**, *32*, 477.
(25) Daniel, C.; Guerra, G. *Soft Mater.* **2004**, *2*, 47.

MA047355D